Journal of Drug Delivery Science and Technology 104 (2025) 106470

Contents lists available at ScienceDirect

Journal of Drug Delivery Science and Technology

journal homepage: www.elsevier.com/locate/jddst

Transdermal delivery of *Acheta domesticus* protein hydrolysate using nanostructured lipid carriers and Derma Stamp – Does the combination of lipid-based formulation and a physical technique add value for permeation and retention?

Kankanit Yeerong [a], Grzegorz Sebastian Czyrski [b], Andrea Heinz [b], Anette Müllertz [c,d], Thomas Rades [c], Wantida Chaiyana [a,e,f,*]

[a] Department of Pharmaceutical Sciences, Faculty of Pharmacy, Chiang Mai University, Chiang Mai, 50200, Thailand
[b] Department of Pharmacy, LEO Foundation Center for Cutaneous Drug Delivery, University of Copenhagen, 2100, Copenhagen, Denmark
[c] Department of Pharmacy, Faculty of Health and Medical Sciences, University of Copenhagen, Universitetsparken 2, 2100, Copenhagen, Denmark
[d] Bioneer: FARMA, Department of Pharmacy, University of Copenhagen, Universitetsparken 4, Copenhagen, 2100, Denmark
[e] Center of Excellence in Pharmaceutical Nanotechnology, Faculty of Pharmacy, Chiang Mai University, Chiang Mai, 50200, Thailand
[f] Multidisciplinary and Interdisciplinary School, Chiang Mai University, Chiang Mai, 50200, Thailand

ARTICLE INFO

Keywords:
Acheta domesticus
Derma Stamp
Microneedles
Nanostructure lipid carriers
Protein hydrolysate
skin permeation
Dermal delivery

ABSTRACT

Acheta domesticus protein hydrolysate (PH) is a natural anti-skin aging compound, but its effectiveness is hindered by poor skin penetration due to its hydrophilicity and high molecular weight. This study aimed to compare the enhancement of PH skin delivery by increasing lipophilicity with nanostructured lipid carriers (NLCs) and bypassing the skin barrier using physical techniques, including Derma Stamp and dissolving microneedles (MNs). Fluorescein isothiocyanate (FITC)-tagged PH was prepared to track the transdermal transport, and complexed with dioctyl sodium sulfosuccinate (DSS) to be encapsulated into NLCs, prepared using a melt emulsification method. Skin delivery was evaluated in terms of skin permeation and skin retention using Franz diffusion cells. The FITC-PH loaded NLCs had a particle size of 238.9 ± 0.8 nm, a polydispersity index of 0.3 ± 0.0, a zeta potential of −23.6 ± 1.0 mV, and an encapsulation efficiency of 65.1 ± 2.1 %. The MNs, prepared with polyvinylpyrrolidone K30 and polyvinyl alcohol (38:15 wt ratio), had uniform sharp needles and a high FITC-PH loading capacity of 97.2 ± 1.9 %. PH permeation was most effectively enhanced through physical barrier bypassing, particularly with the Derma Stamp, followed by MNs and finally due to incorporation into NLCs. Notably, when utilizing the Derma Stamp, converting the aqueous solution of PH into an NLC formulation added positive benefits by significantly improving skin retention. In conclusion, it was suggested that while physical enhancement methods are crucial for permeation of the PH, optimizing formulation characteristics, such as incorporation into NLCs, further increased the overall effectiveness of skin delivery.

1. Introduction

With over 1.3 million species, insects constitute the most abundant group of organisms on earth [1]. Thus, perhaps somewhat surprisingly, insects have only more recently emerged as valuable resources for human nutrition, medicinal applications, and as constituents in cosmetic products. Edible insects provide a valuable protein source, characterized by a beneficial amino acid profile alongside their protein abundance [2]. The house cricket (*Acheta domesticus*) is one of the edible insect species garnering specific attention as a novel protein and nutrient source, promising for the food industry as a safe and environmentally sustainable food option with significant biological value [3]. In addition to its role in the food industry, *A. domesticus* has also demonstrated appealing applications in the cosmetic and cosmeceutical areas. Our previous studies showed that extracts from *A. domesticus* demonstrate anti-skin aging properties, including stimulation of transforming growth factor-beta 1 (TGF-β1) expression, and inhibition of collagenase and hyaluronidase activities [4]. Additionally, bioactive peptides isolated

* Corresponding author. Department of Pharmaceutical Sciences, Faculty of Pharmacy, Chiang Mai University, Chiang Mai, 50200, Thailand.
E-mail address: wantida.chaiyana@cmu.ac.th (W. Chaiyana).

https://doi.org/10.1016/j.jddst.2024.106470
Received 20 October 2024; Received in revised form 14 November 2024; Accepted 1 December 2024
Available online 4 December 2024
1773-2247/© 2024 The Authors. Published by Elsevier B.V. This is an open access article under the CC BY-NC license (http://creativecommons.org/licenses/by-nc/4.0/).

from *A. domesticus* hydrolysate exhibit potent anti-skin aging effects, suggesting their potential as a cosmeceutical ingredient [5]. As protein hydrolysates have become increasingly popular as natural antioxidants due to their ability to release bioactive peptides containing 2–20 amino acid residues through hydrolysis [6], *A. domesticus* protein hydrolysates (PHs) offer a natural solution for anti-skin aging in cosmetic formulations. Nevertheless, a notable challenge persists due to the limited permeation of proteins and protein hydrolysates through the skin, affecting their effectiveness. The difficulty in delivering therapeutic proteins or protein hydrolysates through the skin arises from the natural impermeability of this biological barrier to large and polar molecules. Innovative delivery systems are thus essential to facilitate the efficient transportation of proteins and protein hydrolysates across the skin. Consequently, there has been a growing interest in the development of such delivery systems.

Among the various delivery systems, nanostructured lipid carriers (NLCs) have emerged as promising vehicles to enhance skin permeability and to target bioactive compounds in the skin layer [7]. Additionally, NLCs possess significant potential in both the pharmaceutical and cosmetics markets due to additional beneficial effects such as skin hydration enhancement [8]. NLCs were first developed in the late 1990s as substitutes for solid lipid nanoparticles (SLNs) to prevent cargo molecules from being expelled from the crystalline matrices formed by SLNs [9]. NLCs are structured with a core composed of a blend of solid and liquid lipids, where the solid lipids typically have longer chain lengths compared to the medium to short chains found in liquid lipids or oils [10]. This composition decreases the overall crystallinity of the nano-formulation compared to SLNs and introduces imperfections in the solid matrix, creating small environments for drug encapsulation [11]. As NLCs are known for their versatility in delivering both hydrophilic and lipophilic drugs [8], they may be a promising formulation option to effectively deliver protein hydrolysates derived from *A. domesticus* into and through the skin.

Transdermal permeation can also be enhanced through the application of physical techniques such as the use of ultrasound, iontophoresis, electroporation, magnetophoresis, and microneedles (MNs) [12]. The Derma Stamp, a device equipped with 140 medical-grade stainless steel needles of adjustable length [13], is a commercially available microneedling system. It perforates micron-sized channels through the stratum corneum, allowing both small and large molecules to reach the dermis without activating dermal nerves [14]. However, research comparing its effectiveness in skin permeation and retention, whether used alone or in combination with formulation methods such as lipid-based formulation, is scarce. To simplify the combination of physical techniques and formulations into a single application, dissolving MNs have become a focus of interest [15]. MNs act by perforating the stratum corneum and delivering proteins into the dermis through this minimally invasive route [16,17]. In the cosmetic industry, MNs have demonstrated effectiveness in creating precise channels for the penetration of cosmetic compounds and stimulating the wound repair process of the skin [18].

The present study aimed to compare skin permeation and retention of PH from either a simple aqueous solution or encapsulated into NLCs. In addition, the effect of applying physical techniques (Derma Stamp or MNs) on skin permeation and retention of PH was assessed, again from either a simple aqueous solution or encapsulated into NLCs. The study thus compared skin permeation and retention of PH from a simple aqueous solution and from an NLC formulation when combined with skin pretreatment using the Derma Stamp or a single application of dissolving MNs.

2. Materials and methods

2.1. Insect material

Frozen *A. domesticus* was acquired from the Ruamchok market in Chiang Mai, Thailand. The frozen *A. domesticus* were thawed at ambient temperature and dried using a hot air oven at 45 °C (Memmert, Schwabach, Germany) until a consistent weight was obtained. Subsequently, dried *A. domesticus* were converted into a fine powder using a Moulinex™ blender, model number LM2070BD (Moulinex SA, Bagnolet, France), and stored in a sealed container at −20 °C for further analysis.

2.2. Chemical reagents

Alcalase® enzyme from *Bacillus licheniformis* was purchased from EMD Millipore (Darmstadt, Germany). Dioctyl sulfosuccinate sodium salt (DSS), poly (vinyl alcohol) (PVA) (average molecular weight 85000–124000 g/mol), FluoroTag™ FITC conjugation kit, and polysorbate 80 (Tween® 80) were purchased from Merck KGaA (Darmstadt, Germany). Poly(1-vinyl-2-pyrrolidone) (PVP) K30 (molecular weight of 44000–54000 g/mol) and poloxamer (Kolliphor®) P188 were purchased from BASF (Florham Park, NJ, USA). Caprylic/capric acid triglyceride (Migilyol® 812 N) was a free sample from Cremer Oleo (Hamburg, Germany). Hydrochloric acid (HCl) and phosphate-buffered saline (PBS) tablets, containing 137 mM of sodium chloride (NaCl), 10 mM phosphate buffer, and 2.7 mM potassium chloride (KCl), were purchased from Thermo Fisher Scientific (Waltham, MA, USA). Glyceryl palmitostearate (Precirol® ATO 5) was obtained from Gattefossé (Lyon, France). All experiments utilized purified Milli-Q water obtained from a Milli-Q® Reference Ultrapure Water Purification System from EMD Millipore Corporation (Billerica, MA, USA).

2.3. Preparation of PH

PH was prepared via enzymatic hydrolysis as outlined in a previous study [4]. Briefly, the proteins from *A. domesticus* were precipitated by isoelectric precipitation and then hydrolyzed using enzymatic hydrolysis by Alcalase enzyme. The hydrolysis process was conducted under the following conditions: enzyme-to-substrate concentration: 2.1 % (*w*/*w*), duration: 227 min, temperature: 61.5 °C. The reaction was stopped by heating at 90 °C for 20 min followed by centrifugation at 8000×*g* for 15 min. The PH was obtained by freeze-drying of the supernatant (Christ, Beta 2–8 LD-plus, Osterode am Harz, Germany) with the main drying carried out at a temperature of −75 °C and a pressure of 0.011 mbar for 24 h, and the final drying at −65 °C and 0.054 mbar for 1 h. The PH was stored at −20 °C until analysis.

2.4. Quantitative determination of PH by fluorescence spectroscopy

2.4.1. Preparation of fluorescein isothiocyanate-labeled PH (FITC-PH)

To prevent interference from endogenous proteins and peptides in the porcine ear skin during skin permeation and retention studies, PH was labeled with fluorescein isothiocyanate (FITC). The labeling procedure was conducted using a FluoroTag™ FITC conjugation kit (Sigma, St. Louis, MO, USA), following the manufacturer's instructions. Briefly, PH was dissolved in PBS solution (pH 7.4) at a concentration of 20 mg/mL. Subsequently, 250 μL of 1 mg/mL FITC solution in sodium carbonate-bicarbonate buffer (pH 9.0) was added dropwise to the PH solution under continuous stirring, followed by a 2 h incubation period at room temperature. FITC-labeled PH was then isolated using a Sephadex G-25 column (Bio-Rad Laboratories, CA, USA) with PBS solution as the elution buffer. The collected fractions were monitored for absorbances at 280 nm and 495 nm, and those with A280 values > 0.4 were pooled and dried using a freeze dryer (HT40, Beijer Electronics Products AB, Sweden), yielding FITC-PH (Supplementary data – Fig. S1).

2.4.2. Determination of FITC-PH content by fluorescence spectroscopy

FITC-PH was quantified by fluorescence spectroscopy using the CLARIOstar® Plus multi-mode microplate reader (BMG LabTech, Ortenberg, Germany). Briefly, the freeze-dried FITC-PH was reconstituted in PBS solution (pH 7.4) at various concentrations.

Subsequently, fluorescence measurements were taken using a fluorescence spectrophotometer, with excitation and emission wavelengths set to 495 nm and 525 nm, respectively. A standard curve of FITC-PH was made using concentrations ranging from 0 to 200 μg/mL, yielding the linear equation $y = 1126x + 472$ with an R^2 value of 0.9998. The limit of detection (LOD) was calculated from the standard deviation of the y-intercept (σ) and the slope (S) using the equation LOD = 3.3σ/S, while the limit of quantitation (LOQ) was determined using the equation LOQ = 10σ/S. This resulted in an LOD of 1.38 μg/mL and an LOQ of 4.19 μg/mL. All measurements were conducted in independent triplicates.

2.5. Development of blank NLCs and FITC-PH-DSS in NLCs

2.5.1. Development of blank NLCs

The blank NLCs were developed using a melt emulsification method, following previously described procedures with some modifications [19]. Briefly, an aqueous phase was prepared containing 3 mL of Milli-Q water, 20 mg of Poloxamer P188, and 40 mg of Tween® 80. This aqueous phase was heated at 80 °C for 1 min. Subsequently, the heated aqueous phase was combined with a melted lipid phase consisting of 200 mg of glyceryl palmitostearate and 20 mg of caprylic/capric triglyceride while heating to 85 °C. The mixture was immediately sonicated using a probe sonicator (Q125, Qsonica, Newton, CT, USA) at 80 W for 5 min in 10 s pulse-on and 2 s pulse-off mode. The resulting emulsion was stored at 4 °C to facilitate the NLC formation for 24 h, and then the particles were isolated by centrifugation using a 100 kDa molecular weight cut-off centrifugal filter unit (Amicon® Ultra-4, Merck KGaA, Darmstadt, Germany) at 3500 rpm for 15 min.

2.5.2. Development of FITC-PH-DSS in NLCs

FITC-PH-loaded NLCs were prepared using the melt emulsification method as described in Section 2.5.1. Before incorporation into NLCs, FITC-PH was complexed with dioctyl sulfosuccinate sodium salt (DSS) using a hydrophobic ion pairing method, following the protocol of Claus et al. (2023) [20] with some modifications, to enhance the encapsulation of PH in the NLCs. Briefly, 12.5 mg of FITC-PH were redissolved in a 0.01 N HCl solution (pH 2), followed by the gradual addition of 16.7 mg of DSS solution under continuous stirring for 2 h. Subsequently, the resulting mixture was subjected to freeze drying (LyoQuest Telstar freeze dryer, Azbil Telstar® Technologies, Barcelona, Spain), ultimately producing the FITC-PH-DSS complex. The main drying phase was conducted at −50 °C at 0.1 mbar for 16 h, followed by a final drying phase at 25 °C at 0.1 mbar for 12 h. Subsequently, 12.5 mg of FITC-PH-DSS complex was dispersed into the aqueous phase of the NLCs system, followed by the same procedure used to prepare the blank NLCs, resulting in FITC-PH-DSS in NLCs.

2.5.3. Characterization of blank NLCs and FITC-PH-DSS in NLCs

The blank NLCs and FITC-PH-DSS in NLCs were characterized for their mean particle size (Z-average diameter) and polydispersity index (PDI) using dynamic light scattering (DLS), while the zeta potential was determined by electrophoretic light scattering (ELS) using a Zetasizer Nano ZS (Malvern Instruments Ltd., Malvern, UK), following the protocol of Jiamphun and Chaiyana (2023) [21]. For sample preparation, 1 mL of the NLCs formulation was dispersed in 9 mL of distilled water and measurements were performed at a temperature of 25 °C and a scattering angle of 90°. All experiments were conducted in independent triplicates.

2.5.4. Determination of drug entrapment efficiency of FITC-PH-DSS in NLCs

The encapsulation efficiency of the FITC-PH-DSS in NLCs was indirectly determined by measuring the amount of free FITC-PH-DSS in the filtrate obtained after centrifugation using a 100 kDa molecular weight cut-off centrifugal filter unit (Amicon® Ultra-4, Merck KGaA, Darmstadt, Germany) at 3500 rpm for 15 min [19]. The collected filtrate was analyzed for the FITC-PH amount as described in section 2.4.2. The encapsulation efficiency was calculated using the following equation: % Encapsulation efficiency = (A - B)/A × 100, where A represents the total amount of FITC-PH and B represents the amount of FITC-PH in the filtrate. All experiments were conducted in independent triplicates.

2.6. Evaluation of skin permeation and retention of FITC-PH solution and FITC-PH-DSS in NLCs

2.6.1. Preparation of porcine ear skin

Porcine ears, which are known to possess histological and physiological properties similar to human skin [22], were obtained from a local slaughterhouse. The porcine ears were washed and gently shaved using an electric razor. Subsequently, the ears were soaked in PBS solution and then dermatomed (Zimmer® Dermatome AN, Zimmer Biomet., Warsaw, IN, USA) to a thickness of 600 μm. Subsequently, the dermatomed porcine ear skin was carefully wrapped in aluminum foil and stored at −20 °C for up to three months before further use.

2.6.2. In vitro skin permeation study

FITC-PH solution and FITC-PH-DSS in NLC were evaluated for their skin permeation profile using a Franz diffusion cell following a previous study on intact porcine skin [23]. Frozen dermatomed porcine ear skin was thawed at room temperature for 10 min before use. The dermatomed skin samples were mounted onto the Franz diffusion cells (Phoenix DB-6, Teledyne Technologies, Thousand Oaks, CA, USA) with the stratum corneum side facing the donor part of the cell. The receiver compartments, containing 10 mL of PBS (pH 7.4), were thermostatically maintained at 37 ± 1 °C and stirred with a magnetic bar at 600 rpm. Trans epidermal water loss (TEWL) was measured across the dermatomed skin using an AquaFlux™ Model AF200 (Biox Systems Ltd., London, UK) to confirm skin integrity, and then the skin samples were equilibrated for 30 min. Then, 200 μL of FITC-PH solution or FITC-PH-DSS in NLCs were applied. At pre-determined time points over 24 h (0.5, 1, 2, 4, 6, 8, 12, 24 h), 500 μL samples were withdrawn from the receiver compartment and replaced with an equal volume of PBS solution. The collected samples were centrifuged at 14000 rpm for 10 min and the permeated amounts of FITC-PH were analyzed using fluorescence spectroscopy as described in section 2.4.2. The results are reported as the cumulative amount of FITC-PH permeated after 24 h (Q_{24}, μg/cm^2), steady-state flux (Jss, μg/cm^2/h), and lag time (h). The Jss was determined by plotting the cumulative amount (Q) against time (t) and calculated using the equation: Jss = [dQ/dt]/A, where dQ/dt is the amount of drug permeated per unit time (μg/h) and A is the area of the skin exposed to the drug (cm^2). The lag time was identified as the point where the extended line of the steady-state region intersects the time axis. The experiments were conducted in duplicate.

2.6.3. Skin retention study

The quantification of FITC-PH retained in the dermatomed porcine ear skin was conducted according to a previously established protocol [24]. Following the skin permeation study, the skin samples were gently removed from the diffusion cell and meticulously washed with PBS (pH 7.4) to eliminate any residual samples. Following the cleaning process, the skin samples were cut into smaller pieces and submerged in 1 mL of 50 % (*v/v*) methanol in PBS solution (pH 7.4). After vortexing for 2 min, the samples were subjected to sonication for 30 min using an ultrasonic bath (Elma Schmidbauer GmbH, Singen (Hohentwiel), Germany). Subsequently, the mixtures were subjected to centrifugation at 14000×*g* for 20 min and the supernatant was collected for investigation. The cumulative amounts of FITC-PH in the skin (μg/cm^2) were determined using fluorescence spectrometry, as described in section 2.4.2.

2.7. Treatment of skin with a derma Stamp

The skin was treated with a Derma Stamp using thumb pressure.

Briefly, the dermatomed skin samples were secured on a polystyrene platform and punctured once with the Derma Stamp (âme pure®, CLS Technology SIA, Riga, Latvia) with a needle length of 600 μm using thumb pressure for 30 s. The skin insertion properties of Derma Stamp were assessed using the modified methylene blue-staining method [25]. The perforated porcine ear skin was stretched on a platform, and 50 μL of methylene blue dye was applied to both the epidermis and dermis sides for 30 min. After cleaning off the excess dye, the skin was examined under a digital microscope (DM750, Leica Microsystems GmbH) for stained holes (Supplementary data – Fig. S2). Intact skin was used as control.

2.8. Evaluation of skin permeation and retention of FITC-PH solution and FITC-PH-DSS in NLCs on skin pretreated with a derma Stamp

FITC-PH solution and FITC-PH-DSS in NLCs were investigated for skin permeation and retention on skin pretreated with a Derma Stamp as described in section 2.6. For skin pretreated with the Derma Stamp, the perforated skin samples were mounted on the Franz chambers, and then 200 μL of FITC-PH solution or FITC-PH-DSS in NLCs were applied. The skin permeation results are reported as Q_{24} (μg/cm^2), Jss (μg/cm^2/h), and lag time (t), while the skin retention results are expressed as the cumulative amount of FITC-PH in the skin (μg/cm^2).

2.9. Development of blank MNs, MNs containing FITC-PH, and MNs containing FITC-PH-DSS in NLCs

2.9.1. Fabrication

The blank MNs, MNs containing FITC-PH, and MNs containing FITC-PH-DSS in NLCs were fabricated using a modified micro molding technique following previous studies [25]. PVP K30 was dissolved in Milli-Q water, while PVA was dissolved in Milli-Q water and heated to 90 °C with continuous stirring. For drug-loaded MNs, FITC-PH (5 mg/mL) and FITC-PH-DSS in NLCs (equivalent to 5 mg/mL FITC-PH) were separately dissolved in PVP K30 solution before being combined with PVA solution. Various concentrations of PVA (10 %, 15 %, 20 %, 25 % (*w/w*)) were tested to optimize MN characteristics (Supplementary data – Fig. S3 and Table S1). The mixture blend, consisting of 38 % (*w/w*) PVP K30 and PVA in a 6:4 wt ratio, was centrifuged at 5000 rpm for 5 min and cast into a silicone mold, holding 100 pyramidal MNs (600 μm height, 200 μm base width, and 500 μm interspacing; Micropoint Technologies, Pioneer Junction, Singapore), and then centrifuged again at 5000 rpm for 20 min at 25 °C. After drying at 37 °C for 24 h, the MNs were carefully removed and stored in a sealed container covered with aluminum foil until further use.

2.9.2. Characterization of MNs

The morphologies of blank MNs, MNs containing FITC-PH, and MNs containing FITC-PH-DSS in NLCs were examined using a digital microscope (DM750, Leica Microsystems GmbH, Wetzlar, Germany). The dimensions of MNs were measured with LASX Office software version 1.4.6 28433 (Leica Microsystems GmbH, Wetzlar, Germany). Dissolution profiles of the MNs were evaluated using the method of Aung et al. (2023) on dermatomed skin, equilibrated for 30 min in PBS solution (pH 7.4). The MNs were manually inserted into the skin with thumb pressure for 30 s. The needle heights of the MNs were measured before and at specific intervals (0, 1, 5, 10, and 15 min) using a digital microscope (Supplementary data – Fig. S4). All experiments were performed in duplicate.

Skin insertion properties were assessed using a modified methylene blue-staining method as described in section 2.7 [25] (Supplementary data – Fig. S5). The results are reported as percentage of penetration efficiency, calculated using the following equation: Penetration efficiency (%) = A/B × 100, where A is the number of stained holes and B is the total number of needles. Mechanical properties were evaluated using a texture analyzer following the method of Aung et al. (2023) [26]. The results are expressed as the percentage reduction in needle height, calculated using the following equation: Reduction of the needle height (%) = (A – B)/A × 100; where A represents the initial needle height and B represents the needle height after applying the compression force (Supplementary data – Fig. S6). All experiments were performed in duplicate.

The drug loading of the MN arrays containing FITC-PH and FITC-PH-DSS in NLCs was quantified using fluorescence spectrophotometry as described in section 2.4.2. Initially, MNs containing FITC-PH and FITC-PH-DSS in NLCs were dissolved in 10 mL of PBS (pH 7.4), stirred at 500 rpm for 30 min, and then centrifuged at 5000 rpm for 10 min at 25 °C. A 100 μL aliquot of the supernatant was analyzed for FITC-PH content. Drug loading was calculated using the formula: Drug loading (%) = A/B × 100; where A represents the actual amount of FITC-PH and B represents the initial amount of FITC-PH. All experiments were performed in duplicate with three technical repeats per experiment.

2.10. Evaluation of skin permeation and retention of FITC-PH solution and FITC-PH-DSS in NLCs on pretreated skin with derma Stamp versus MNs containing FITC-PH

MNs containing FITC-PH and applications of FITC-PH solution or FITC-PH-DSS in NLCs on intact skin or pretreated skin with Derma Stamp were investigated for skin permeation and retention as described in sections 2.6 and 2.7. In the case of skin treated with the MN arrays, the MN arrays containing FITC-PH were inserted into the skin using thumb pressure for 30 s and the skin samples were then immediately attached to the donor compartment of each cell. The skin permeation results are reported as Q_{24} (μg/cm^2), Jss (μg/cm^2/h), and lag time (h), while the skin retention result is expressed as the cumulative amount of FITC-PH in the skin (μg/cm^2).

2.11. Statistical analysis

All results are presented as mean ± standard deviation (SD) from at least two independent experiments with three technical repeats per experiment. Statistical analysis was conducted using a Mann-Whitney *U* test or Kruskal-Wallis test with GraphPad Prism version 8.0 (GraphPad Software Inc., La Jolla, CA, USA). Significance is indicated when $p < 0.05$.

3. Results and discussion

3.1. Characterization of blank and FITC-PH-DSS in NLCs

Overcoming the stratum corneum presents a significant challenge in achieving effective transdermal delivery of proteins or peptides [27]. To tackle this hurdle, NLC dispersions were developed to enhance transdermal drug delivery (Fig. 1). Visually, the blank NLCs appeared homogeneous, viscous and resembled milk with no precipitates (Fig. 1a). The NLCs had an average particle size of 180.7 nm ± 1.9 nm, PDI of 0.3 ± 0.0, and a zeta potential of −11.2 mV ± 0.4 mV. This suggests that they are nano-scale particles, that could enhance dermal transport efficiency [28]. Although the zeta potential did not fall within the range of lower than −30 mV or higher than +30 mV, the system maintained its physical stability over 24 h. When FITC-PH was complexed with DSS and incorporated into the NLCs, the formulation displayed a yellowish appearance resembling the color of FITC-PH (Fig. 1b). Furthermore, there was a substantial increase in particle size to a mean diameter of 238.9 nm ± 0.8 nm, a PDI of 0.3 ± 0.0, and a pronounced negative zeta potential of −23.6 mV ± 1.0 mV. The increase in particle size suggests successful encapsulation of FITC-PH-DSS in the NLCs, while the decrease in zeta potential may be attributed to the properties of DSS, a negatively charged anionic surfactant [29]. However, the encapsulation efficiency of the FITC-PH-DSS in NLCs was found to be fairly low (65.1 % ± 2.1 %). Despite the potential to improve the encapsulation efficiency of

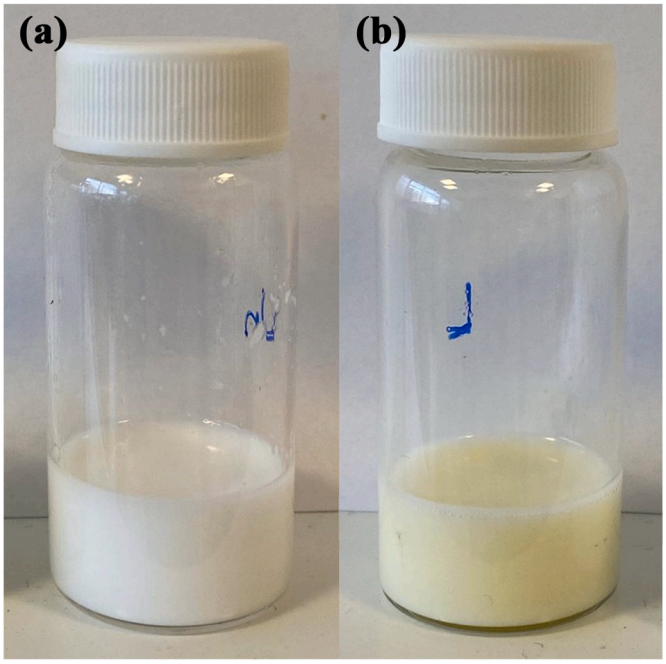

Fig. 1. Physical appearance of (a) blank NLCs and (b) FITC-PH-DSS in NLCs.

hydrophilic molecules in lipid-based nano delivery systems through hydrophobic ion pairing, it is important to note that the natural source PH comprises a wide range of peptides [4]. Some peptides may not be positively charged and therefore not effectively complexed solely with DSS, resulting in charged complexes that still were water-soluble and incompatible with lipid-based systems, leading to a lower encapsulation efficiency overall. However, a particle size of approximately 300 nm or below has been described previously to deliver its contents into the deeper layers of the skin [30]. Therefore, the FITC-PH-DSS in NLCs were utilized for skin permeation and retention studies.

3.2. Comparison of skin permeation and retention between FITC-PH solution and FITC-PH-DSS in NLCs on intact skin

The skin permeation and retention profiles of FITC-PH solution were compared to FITC-PH-DSS in NLCs on intact skin and the results are reported in Table 1. The application of FITC-PH solution on intact skin showed negligible permeation into the receiver compartment throughout the study period, indicating its inability to penetrate the skin. However, the application of FITC-PH-DSS in NLCs into intact skin exhibited detectable permeation after 2 h, extending to 24 h with a minimal Q_{24} of 133.5 ± 10.7 μg/cm^2. It is likely that NLCs enhanced the FITC-PH permeation due to their small particle size and lipophilicity. NLCs comprised of lipid materials resembling those found in skin have been shown to promote dissolution and release of the encapsulated drug, leading to improved topical, dermal, as well as systemic effects [31]. Additionally, the small size of NLCs provides a large surface area upon skin contact, enhancing occlusion and facilitating drug penetration into the skin [32]. The results of this study are consistent with a previous study demonstrating the permeation of DPK-060, a synthetic 17 amino acid peptide for treating atopic dermatitis, from an NLC gel, which was found to be 3-fold higher after 12 h when compared to conventional DPK-060 gel and lotion [32]. Additionally, penetrating deeper skin layers is crucial for the effectiveness of the anti-skin aging compounds in the PH [33]. This is due to the fact that the PH target cells, i.e., fibroblasts or keratinocytes, are predominantly located in the basal layer of the epidermis or even deeper in the dermis [34]. Thus, ensuring successful penetration through the outer skin layers is necessary for PH to effectively exert its desired effect on skin aging. The skin retention results of this study revealed that the application of either FITC-PH solution or FITC-PH-DSS in NLCs on intact skin resulted in the retention of an insignificant amount of FITC-PH, indicating that FITC-PH was unable to penetrate the skin.

Table 1
Skin permeation and retention parameters after application of FITC-PH solution and FITC-PH-DSS in NLCs (n = 2).

Treatment	Skin permeation parameters			Skin retention parameter
	Q_{24} (μg/cm^2)	Jss (μg/cm^2/h)	Lag time (h)	Cumulative amounts of FITC-PH in skin (μg/cm^2)
Application of FITC-PH solution on intact skin	12.6 ± 8.3^b	N.D.	N.D.	4.5 ± 1.4^a
Application of FITC-PH-DSS in NLCs on intact skin	133.5 ± 10.7^a	6.9 ± 0.8	2.3 ± 0.0	11.4 ± 5.9^a

FITC = fluorescein isothiocyanate, PH = *A. domesticus* protein hydrolysate, DSS = dioctyl sulfosuccinate sodium salt, NLCs = nanostructured lipid carriers, Q_{24} = cumulative amount of FITC-PH permeating at 24 h, Jss = steady-state flux, and h = hour. The data are shown as mean ± SD. The lowercase letters (a and b) indicate significant differences among the treatments. Statistical significance was analyzed using a Mann-Whitney *U* test ($p < 0.05$).

3.3. Comparison of skin permeation and retention between FITC-PH solution and FITC-PH-DSS in NLCs on intact skin and skin pretreated with derma Stamp

FITC-PH solution and FITC-PH-DSS in NLCs were compared for skin permeation and retention on intact skin and skin pretreated with a Derma Stamp. The results were shown in Table 2. The dermatomed skin, treated with a Derma Stamp, showed perforation in the epidermis but not in the dermis (Supplementary data – Fig. S2). It can be inferred that not the entire length of the needles penetrated the skin. The pretreatment of the skin by a Derma Stamp followed by the application of FITC-PH solution or FITC-PH-DSS in NLCs proved to even further enhance FITC-PH permeation, achieving Q_{24} values of 652.6 ± 58.0 μg/cm^2 and 596.9 ± 66.0 μg/cm^2, respectively. This is due to the ability of the Derma Stamp to generate micropores in the skin facilitating the diffusion of FITC-PH [35]. It is worth mentioning that no statistically significant difference in Q_{24} was observed between the application of either

Table 2
Skin permeation and retention parameters after application of FITC-PH solution and FITC-PH-DSS in NLCs after pretreatment of the skin using a Derma Stamp (n = 2).

Treatment	Skin permeation parameters			Skin retention parameter
	Q_{24} (μg/cm^2)	Jss (μg/cm^2/h)	Lag time (h)	Cumulative amounts of FITC-PH in skin (μg/cm^2)
Application of FITC-PH solution after Derma Stamp pretreatment of the skin	652.6 ± 58.0^a	30.0 ± 3.2^a	2.9 ± 1.2^a	161.3 ± 5.5^b
Application of FITC-PH-DSS in NLCs after Derma Stamp pretreatment of the skin	596.9 ± 66.0^a	27.3 ± 5.4^a	2.4 ± 0.4^a	234.0 ± 21.6^a

FITC = fluorescein isothiocyanate, PH = *A. domesticus* protein hydrolysate, DSS = dioctyl sulfosuccinate sodium salt, NLCs = nanostructured lipid carriers, Q_{24} = cumulative amount of FITC-PH permeating at 24 h, Jss = steady-state flux, and h = hour. The data are shown as mean ± SD. The lowercase letters (a and b) indicate significant differences among the treatments. Statistical significance was analyzed using a Mann-Whitney *U* test ($p < 0.05$).

FITC-PH solution or FITC-PH-DSS in NLCs after pretreatment of the skin using a Derma Stamp. Skin perforation reduces the barrier function of the stratum corneum, allowing rapid diffusion of substances into deeper skin layers and receptor fluid [36,37]. Additionally, higher Jss values ($p < 0.05$) were observed after pre-treating the skin with a Derma Stamp, followed by application of either a FITC-PH solution or FITC-PH-DSS in NLCs as compared to intact skin. Moreover, perforating the skin samples with the Derma Stamp techniques showed significantly higher FITC-PH retention in the skin ($p < 0.05$) than in intact skin. However, the lag time for all samples showed no significant difference ($p > 0.05$). These findings confirm that the skin perforation allowed FITC-PH to pass through the stratum corneum and reach directly into the deeper layers of the skin. Notably, the skin pretreated with Derma Stamp followed by application of FITC-PH-DSS in NLCs retained more FITC-PH than FITC-PH solution applied after pretreating the skin with the Derma Stamp ($p < 0.05$), with 234.0 ± 21.6 μg/cm^2 and 161.3 ± 5.5 μg/cm^2 after 24 h, respectively [38]. A likely explanation is that the lipid matrices in NLCs form a sustained-release depot at the site of action in the skin, enabling controlled release of FITC-PH-DSS, which reduces rapid clearance and leads to higher skin retention. However, this requires further investigations. Additionally, it was observed that the findings from skin pretreated with a Derma Stamp were distinctly different from those of intact skin, as the NLCs, used as a nano delivery system beneficial for delivering FITC-PH to intact skin, were not essential when the skin was perforated, allowing the hydrophilic FITC-PH to penetrate directly. However, the combination of NLCs and the Derma Stamp resulted in significantly higher skin retention, suggesting that the NLCs were beneficial for retaining the hydrophilic FITC-PH in the skin layers. The results of this study are consistent with previous studies demonstrating that combining invasomes with Dermaroller® treatment increased the amounts of radiolabeled mannitol in the stratum corneum and receptor fluid [36]. Therefore, this study shows that combining skin perforation using a Derma Stamp and subsequent application of a lipid-based nano delivery system (NLCs) effectively facilitates the permeation and deposition of FITC-PH in the skin.

3.4. Development and characterization of blank MNs, MNs containing FITC-PH, and MNs containing FITC-PH-DSS in NLCs

The blank MNs produced with various PVA concentrations were developed and the impact of the PVA concentration on the morphology of the MNs is illustrated in Fig. S3. The dimensions and characteristics of the blank MNs are shown in Table S1, as well as in Figs. S4 and S5. Due to their rapid dissolution rate, effective skin piercing, and robustness, the MNs formulated with 38 % (*w/w*) of PVP K30 and 15 % (*w/w*) of PVA were selected for incorporation of FITC-PH and FITC-PH-DSS in NLCs. The morphology of blank MNs, MNs containing FITC-PH, and MNs containing FITC-PH-DSS in NLCs are presented in Fig. 2, and their dimensions and characteristics are described in Table 3. The external appearance of MNs containing FITC-PH resembled the blank MNs, appearing yellowish-transparent and homogeneous with good structural integrity, comprising a 10 × 10 sharp, perfectly formed needles. MNs containing FITC-PH-DSS in NLCs displayed a yellowish-milky and non-homogeneous appearance throughout the patch. This may be attributed to insufficient pressure applied to fill the polymer and lipid-based system into the molds, with previous studies suggesting alternative methods for fabricating lipid-based delivery systems loaded into MNs, such as using positive pressure chambers or lithography methods [39,40].

Additionally, the blank MNs and MNs containing FITC-PH completely dissolved within 15 min after insertion into dermatomed porcine ear skin. However, MNs containing FITC-PH-DSS in NLCs required 30 min to completely dissolve. This variation in dissolution ability might stem from the lipophilicity of NLCs [41]. The presence of FITC-PH did not alter the skin insertion profile of MNs, with a

Table 3
Dimensions and characteristics of blank MNs, MNs containing FITC-PH, and MNs containing FITC-PH-DSS in NLCs (n = 2).

Characteristics	Blank MNs	MNs containing FITC-PH	MNs containing FITC-PH-DSS in NLCs
Average needle height (μm)	538.8 ± 1.3[a]	535.8 ± 2.1[a]	538.4 ± 0.6[a]
Skin dissolution profile (Dissolution time)	Within 15 min	Within 15 min	Within 30 min
Skin insertion profile (% Penetration efficiency)	99.5 ± 0.7[a]	98.5 ± 0.7[a]	90.5 ± 0.7[b]
Mechanical property (% Needle height reduction)	4.5 ± 0.8[b]	8.1 ± 0.2[a]	Broken
% Drug loading	–	97.2 ± 1.9	–

MNs = microneedles, FITC = fluorescein isothiocyanate, PH = *A. domesticus* protein hydrolysate, DSS = dioctyl sulfosuccinate sodium salt, and NLCs = nanostructured lipid carriers. The data are shown as mean ± SD. The lowercase letters (a and b) indicate significant differences between the MN samples. Statistical significance was assessed using the Mann-Whitney *U* test or Kruskal-Wallis test ($p < 0.05$).

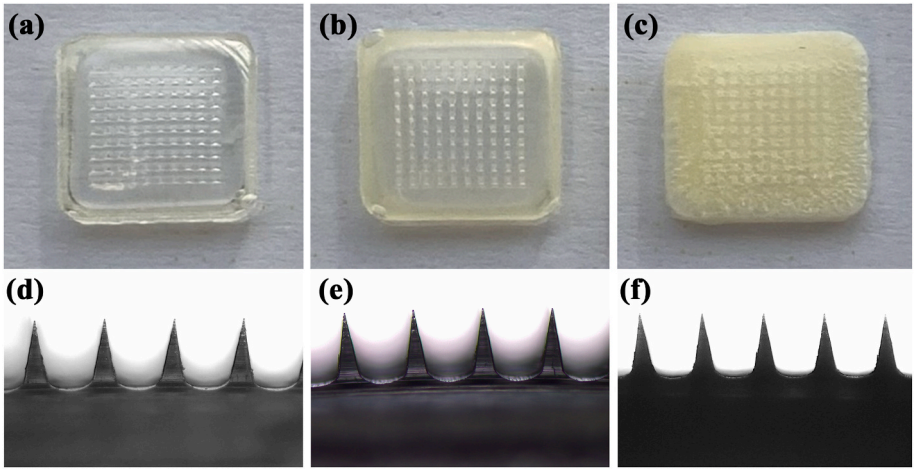

Fig. 2. External appearance of (a) blank microneedles (MNs), (b) MNs containing fluorescein thiocyanate-labeled *A. domesticus* protein hydrolysate (FITC-PH), and (c) MNs containing FITC-PH complexed with dioctyl sulfosuccinate sodium salt (DSS) loaded in nanostructured lipid carriers (NLCs), and morphology under the digital microscope of (d) blank MNs, (e) MNs containing FITC-PH, and (f) MNs containing FITC-PH-DSS in NLCs.

penetration efficiency percentage of 99.5 % ± 0.7 %. However, MNs containing FITC-PH-DSS in NLCs displayed a reduced penetration efficiency ability of 90.5 % ± 0.7 %. Furthermore, the mechanical properties of the MNs containing FITC-PH are significantly different from the blank MNs, with a height reduction of 8.1 % ± 0.2 % as compared to 4.5 % ± 0.8 % for the blank MNs. It is likely that the presence of FITC-PH influenced the mechanical properties of the MNs, as previously reported for other compounds [41,42], however, they retained sufficient mechanical strength to cross the stratum corneum barrier. On the other hand, MNs containing FITC-PH-DSS in NLCs broke when a force of 32 N was applied. This suggests that the addition of NLCs weakened the mechanical strength of the MNs due to incompatibility between the lipidic system and the polymer, especially with high lipid loading [40]. Therefore, the MNs containing FITC-PH-DSS in NLCs were excluded from further experiments due to the weakened structure. The MNs containing FITC-PH possessed a high drug loading capacity of 97.2 % ± 1.9 %. This is in line with a previous study showing that MNs made with 15 % (*w/w*) PVA and 20 % (*w/w*) PVP incorporated 94 μg ± 15 μg of ovalbumin per array from an initial 100 μg [43]. Taken together, FITC-PH was successfully encapsulated into MNs composed of 38 % (*w/w*) PVP K30 and 15 % (*w/w*) PVA, which exhibited excellent skin insertion capability, skin dissolution ability, and mechanical strength. Therefore, the MNs were further investigated for their skin permeation and retention properties.

3.5. Comparison of skin permeation and retention between MNs containing FITC-PH and application of FITC-PH solution or FITC-PH-DSS in NLCs on skin pretreated with derma Stamp

MNs containing FITC-PH were investigated for skin permeation and skin retention profile on intact skin and skin pretreated with the Derma Stamp (Fig. 3). Notably, bypassing the physical barrier effectively enhanced the skin permeation and skin retention of PH compared to the use of NLCs. Although NLCs exhibited greater efficacy in enhancing skin permeation on intact skin, their effectiveness diminished for skin pretreated with the Derma Stamp. The micro-channels created by the Derma Stamp facilitate direct access for the PH to deeper layers of the skin, thus lowering the reliance on increasing lipophilicity for permeation. Thus, the additional benefits of NLCs are not pronounced. MNs containing FITC-PH significantly increased permeated FITC-PH amounts (202.2 ± 35.8 μg/cm^2), steady state flux (16.9 ± 7.7 μg/cm^2/h), and cumulative retained FITC-PH amount in skin (100.6 ± 17.0 μg/cm^2) compared to the application of FITC-PH-DSS in NLCs on intact skin but less than the application of FITC-PH solution or FITC-PH-DSS in NLCs after pretreatment by Derma Stamp. This can be attributed to only the parts of the MN arrays that are dissolving, which are allowing the release and penetration of FITC-PH into the skin, while some of FITC-PH remained entrapped within the remaining MN array base upon removal [44], resulting in a prolonged release pattern from the MNs. The results are consistent with Lee's study [45], which found that PVP/PVA MNs provided sustained release, with the transdermal delivery rate regulated by the PVP/PVA ratio. Additionally, the variability of the Jss values observed in the skin treated with FITC-PH-loaded MNs (Jss of 16.9 ± 7.7 μg/cm^2/h), which was accompanied by a high standard deviation (SD), might be attributed to variation in the diffusivity and degradation rate of the polymer [46]. Microneedling by using both the Derma Stamp and MNs offers several advantages, including being a simple, safe, effective, and minimally invasive therapeutic technique [47]. The dissolving MNs, which encapsulate the drug, fully dissolve in the skin, producing no sharp waste, while the Derma Stamp creates small punctures in the skin before the formulation is applied. However, high-tech equipment is required to fabricate the MNs, whereas the Derma Stamp device is simpler to produce, resulting in higher production costs for microneedles. Moreover, difficulties in precisely manufacturing microneedles with sophisticated microstructures still strongly hinder their practical applications [48]. The findings of the current study suggest that using the Derma Stamp offers greater benefits compared to using the MNs together with the FITC-PH solution or NLCs, respectively.

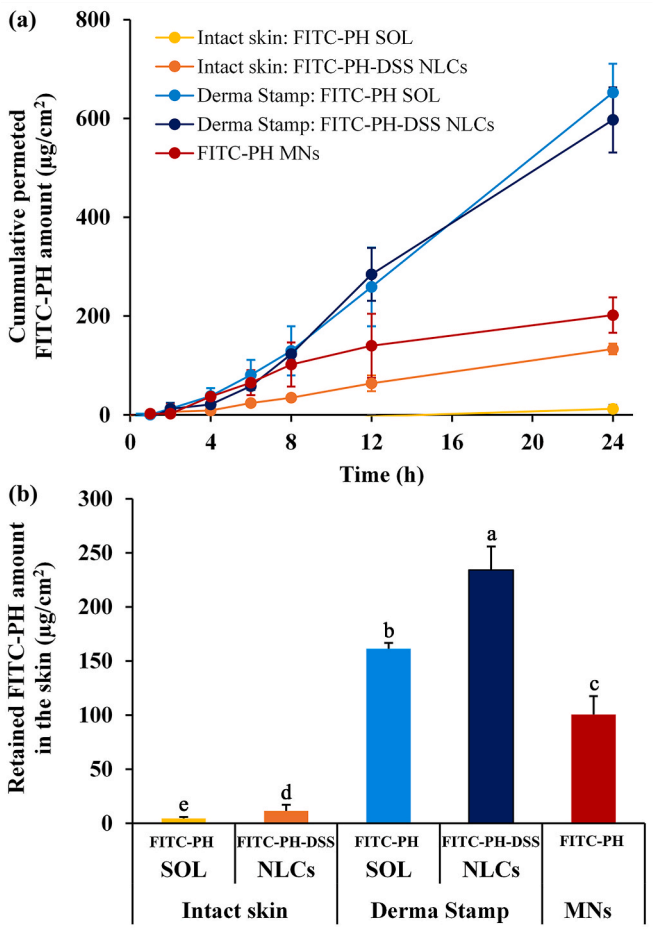

Fig. 3. Skin permeation profiles (a) and skin retention (b) of FITC labeled *A. domesticus* protein hydrolysate solution (FITC-PH SOL) into intact skin (yellow color), FITC-PH complexed with dioctyl sulfosuccinate sodium salt loaded in nanostructured lipid carriers (FITC-PH-DSS NLCs) into intact skin (orange color), FITC-PH solution after Derma Stamp pretreatment of the skin (light blue color), FITC-PH-DSS complex-loaded NLCs after Derma Stamp pretreatment of the skin (dark blue color), and FITC-PH from MNs formulated with 38 % (*w/w*) of poly(1-vinyl-2-pyrrolidone) K30 and 15 % (*w/w*) of poly (vinyl alcohol) (FITC-PH MNs) (red color) over 24 h. Different letters (a, b, c, d, and e) denote statistically significant differences in skin retention, as determined by Kruskal-Wallis test using GraphPad Prism version 8.0 ($p < 0.05$). (For interpretation of the references to color in this figure legend, the reader is referred to the Web version of this article.)

4. Conclusion

In this study, a bioactive protein hydrolysate from *A. domesticus* (PH) was labeled with FITC, complexed with DSS, and incorporated into the NLCs. NLCs enhanced skin permeation of FITC-PH compared to a solution on intact skin. Moreover, combining FITC-PH-DSS in NLCs with a physical technique (Derma Stamp) further increased skin permeation and retention. MNs containing FITC-PH-DSS in NLCs exhibited breakage under specific compression forces. In permeation and retention studies on porcine skin, MNs containing FITC-PH improved skin permeation and retention compared to applying FITC-PH-DSS in NLCs on intact skin, though they were less effective than pretreatment of skin with a Derma Stamp followed by applying the FITC-PH solution and FITC-PH-DSS in NLCs. In conclusion, NLCs enhance the skin permeation of PH compared

to solution. On the other hand, the Derma Stamp dramatically enhanced skin permeation of both the FITC-PH solution and FITC-PH-DSS in NLCs, yielding comparable results. However, the combination of NLCs with the Derma Stamp provided additional benefits by significantly improving skin retention compared to the PH solution alone. These findings indicate that the physical enhancement methods were more effective for delivering PH into the skin compared to lipid nanoparticles. While physical enhancement methods are essential for PH permeation, lipophilicity enhancement of the formulation further enhances skin delivery effectiveness. Future studies should focus on refining lipid-based formulations and preparation methods for incorporating PH into MNs to achieve more robust MNs containing lipid formulations.

CRediT authorship contribution statement

Kankanit Yeerong: Writing – original draft, Validation, Methodology, Investigation, Funding acquisition, Formal analysis, Data curation, Conceptualization. **Grzegorz Sebastian Czyrski:** Writing – review & editing, Writing – original draft, Formal analysis. **Andrea Heinz:** Writing – review & editing, Writing – original draft, Supervision, Resources, Formal analysis, Conceptualization. **Anette Müllertz:** Writing – review & editing, Writing – original draft, Supervision, Resources, Formal analysis, Conceptualization. **Thomas Rades:** Writing – review & editing, Writing – original draft, Supervision, Resources, Formal analysis, Conceptualization. **Wantida Chaiyana:** Writing – review & editing, Writing – original draft, Visualization, Supervision, Resources, Methodology, Conceptualization.

Declaration of competing interest

The authors declare that they have no known competing financial interests or personal relationships that could have appeared to influence the work reported in this paperThe authors declare the following financial interests/personal relationships which may be considered as potential competing interests.

Acknowledgment

This research was funded by the Royal Golden Jubilee Ph.D. Program (RGJ-Ph.D. Program), Thailand, grant number PHD/0118/2561. The APC was funded by the Center of Excellence in Pharmaceutical Nanotechnology, Faculty of Pharmacy, Chiang Mai University, Chiang Mai, Thailand. The work was further supported by the LEO Foundation, Denmark, Grants 15007 (AH) and LF-ST-21-500005 Project 1 (TR, GSC).

Appendix A. Supplementary data

Supplementary data to this article can be found online at https://doi.org/10.1016/j.jddst.2024.106470.

Data availability

Data will be made available on request.

References

[1] W. Kim, J. Yung, Y. Chung, Research on the value of crickets as ingredients for cosmetics, Int. J. High Sch. Res. 5 (3) (2023) 125–130, https://doi.org/10.36838/v5i3.21.
[2] A.B. Nongonierma, R.J. FitzGerald, Unlocking the biological potential of proteins from edible insects through enzymatic hydrolysis: a review, Innov. Food Sci. Emerg. Technol. 43 (2017) 239–252, https://doi.org/10.1016/j.ifset.2017.08.014.
[3] G. Pilco-Romero, A.M. Chisaguano-Tonato, M.E. Herrera-Fontana, L.F. Chimbo-Gándara, M. Sharifi-Rad, F. Giampieri, M. Battino, M.G. Vernaza, J.M. Álvarez-Suárez, House cricket (*Acheta domesticus*): a review based on its nutritional composition, quality, and potential uses in the food industry, Trends Food Sci 142 (2023) 104226, https://doi.org/10.1016/j.tifs.2023.104226.
[4] K. Yeerong, P. Chantawannakul, S. Anuchapreeda, S. Wangtueai, W. Chaiyana, Optimization of hydrolysis conditions, isolation, and identification of biologically active peptides derived from *Acheta domesticus* for antioxidant and collagenase inhibition, Antioxidants 13 (2024) 367, https://doi.org/10.3390/antiox13030367.
[5] K. Yeerong, P. Chantawannakul, S. Anuchapreeda, T. Rades, A. Müllertz, W. Chaiyana, *Acheta domesticus*: a natural source of anti-skin-aging ingredients for cosmetic applications, Pharmaceuticals 17 (2024) 346, https://doi.org/10.3390/ph17030346.
[6] Q. Zhang, X. Tong, B. Qi, Z. Wang, Y. Li, X. Sui, L. Jiang, Changes in antioxidant activity of Alcalase-hydrolyzed soybean hydrolysate under simulated gastrointestinal digestion and transepithelial transport, J. Funct.Foods 42 (2018) 298–305, https://doi.org/10.1016/j.jff.2018.01.017.
[7] C. Viegas, A.B. Patrício, J.M. Prata, A. Nadhman, P.K. Chintamaneni, P. Fonte, Solid lipid nanoparticles *vs.* nanostructured lipid carriers: a comparative review, Pharmaceutics 15 (2023) 1593, https://doi.org/10.3390/pharmaceutics15061593.
[8] I. Chauhan, M. Yasir, M. Verma, A.P. Singh, Nanostructured lipid carriers: a groundbreaking approach for transdermal drug delivery, Adv. Pharm. Bull. 10 (2020) 150–165, https://doi.org/10.34172/apb.2020.021.
[9] R.H. Müller, M. Radtke, S.A. Wissing, Solid lipid nanoparticles (SLN) and nanostructured lipid carriers (NLC) in cosmetic and dermatological preparations, Adv. Drug Deliv. Rev. 54 (2002) S131–S155, https://doi.org/10.1016/s0169-409x(02)00118-7.
[10] K.L. López, A. Ravasio, J.V. González-Aramundiz, F.C. Zacconi, Solid lipid Nanoparticles (SLN) and nanostructured lipid carriers (NLC) prepared by microwave and ultrasound-assisted synthesis: promising green strategies for the nanoworld, Pharmaceutics 15 (2023) 1333, https://doi.org/10.3390/pharmaceutics15051333.
[11] Y. Ye, J. Yu, D. Wen, A.R. Kahkoska, Z. Gu, Polymeric microneedles for transdermal protein delivery, Adv. Drug Deliv. Rev. 127 (2018) 106–118, https://doi.org/10.1016/j.addr.2018.01.015.
[12] R.S. Vaseem, A. D'cruz, S. Shetty, A. Vardhan, S. Shenoy, S.M. Marques, L. Kumar, R. Verma, Transdermal drug delivery systems: a focused review of the physical methods of permeation enhancement, Adv. Pharm. Bull. 14 (1) (2023) 67, https://doi.org/10.34172/apb.2024.018.
[13] S. Cakmak, One step fabrication of hollow and highly flexible polydimethylsiloxane microneedles, Hittite J. Sci. Eng. 9 (3) (2022) 219–224, https://doi.org/10.17350/hjse19030000274.
[14] A.H. Sabri, Z. Cater, J. Ogilvie, D.J. Scurr, M. Marlow, J. Segal, Characterisation of mechanical insertion of commercial microneedles, J. Drug Deliv. Sci. Technol. 58 (2020) 101766, https://doi.org/10.1016/j.jddst.2020.101766.
[15] C.H. Kumari, N.S. Rao, S.K. Begham, S.S. Babu, G.D. Rao, K.V. Rao, Formulation techniques of lipid based nanoparticles: SLN/NLCs, its evaluation and applications, Int. J. Res. Pharm. Chem. 10 (2020) 111–124.
[16] R. Jamaledin, C. Di Natale, V. Onesto, Z.B. Taraghdari, E.N. Zare, P. Makvandi, R. Vecchione, P.A. Netti, Progress in microneedle-mediated protein delivery, J. Clin. Med. 9 (2) (2020) 542, https://doi.org/10.3390/jcm9020542.
[17] C.L. Caudill, J.L. Perry, S. Tian, J.C. Luft, J.M. DeSimone, Spatially controlled coating of continuous liquid interface production microneedles for transdermal protein delivery, J. Control. Release. 284 (2018) 122–132, https://doi.org/10.1016/j.jconrel.2018.05.042.
[18] J. Yang, X. Liu, Y. Fu, Y. Song, Recent advances of microneedles for biomedical applications: drug delivery and beyond, Acta Pharm. Sin. B 9 (2019) 469–483, https://doi.org/10.1016/j.apsb.2019.03.007.
[19] I. Garcia-Orue, G. Gainza, C. Girbau, R. Alonso, J.J. Aguirre, J.L. Pedraz, M. Igartua, R.M. Hernandez, LL37 loaded nanostructured lipid carriers (NLC): a new strategy for the topical treatment of chronic wounds, Eur. J. Pharm. Biopharm. 108 (2016) 310–316, https://doi.org/10.1016/j.ejpb.2016.04.006.
[20] V. Claus, M. Sandmeier, N. Hock, H. Spleis, S. Lindner, M. Kalb, A. Bernkop-Schnürch, Counterion optimization for hydrophobic ion pairing (HIP): unraveling the key factors, Int. J. Pharm. 647 (2023) 123507, https://doi.org/10.1016/j.ijpharm.2023.123507.
[21] S. Jiamphun, W. Chaiyana, Enhancing skin delivery and stability of vanillic and ferulic acids in aqueous enzymatically extracted glutinous rice husk by nanostructured lipid carriers, Pharmaceutics 15 (2023) 1961, https://doi.org/10.3390/pharmaceutics15071961.
[22] I.P. Dick, R.C. Scott, Pig ear skin as an in-vitro model for human skin permeability, J. Pharm. Pharmacol. 44 (1992) 640–645, https://doi.org/10.1111/j.2042-7158.1992.tb05485.x.
[23] N.N. Aung, T. Ngawhirunpat, T. Rojanarata, P. Patrojanasophon, B. Pamornpathomkul, P. Opanasopit, Fabrication, characterization and comparison of α-arbutin loaded dissolving and hydrogel forming microneedles, Int. J. Pharm. 586 (2020) 119508, https://doi.org/10.1016/j.ijpharm.2020.119508.
[24] E. Larrañeta, J. Moore, E.M. Vicente-Pérez, P. González-Vázquez, R. Lutton, A. D. Woolfson, R.F. Donnelly, A proposed model membrane and test method for microneedle insertion studies, Int. J. Pharm. 472 (2014) 65–73, https://doi.org/10.1016/j.ijpharm.2014.05.042.
[25] G. Li, A. Badkar, S. Nema, C.S. Kolli, A.K. Banga, *In vitro* transdermal delivery of therapeutic antibodies using maltose microneedles, Int. J. Pharm. 368 (2009) 109–115, https://doi.org/10.1016/j.ijpharm.2008.10.008.
[26] N.N. Aung, S. Pengnam, T. Ngawhirunpat, T. Rojanarata, P. Patrojanasophon, P. Opanasopit, B. Pamornpathomkul, Fabrication of polyvinyl pyrrolidone-K90/Eudragit RL100-based dissolving microneedle patches loaded with alpha-arbutin and resveratrol for skin depigmentation, Biomater. Sci. 11 (2023) 4583–4601, https://doi.org/10.1039/D3BM00132F.
[27] H. Katsumi, Y. Tanaka, K. Hitomi, S. Liu, Y.S. Quan, F. Kamiyama, T. Sakane, A. Yamamoto, Efficient transdermal delivery of alendronate, a nitrogen-containing bisphosphonate, using tip-loaded self-dissolving microneedle arrays for the

treatment of osteoporosis, Pharmaceutics 9 (2017) 29, https://doi.org/10.3390/pharmaceutics9030029.
[28] A.Z. Alkilani, H. Abo-Zour, H.A. Basheer, H. Abu-Zour, R.F. Donnelly, Development and evaluation of an innovative approach using niosomes based polymeric microneedles to deliver dual antioxidant drugs, Polymers 15 (2023) 1962, https://doi.org/10.3390/polym15081962.
[29] C. Dumont, V. Jannin, C. Miolane, Q. Lelong, J.P. Valour, S. Urbaniak, H. Fessi, S. Bourgeois, A proof-of-concept for developing oral lipidized peptide nanostructured lipid carrier formulations, J. Drug Deliv. Sci. Technol. 54 (2019) 101394, https://doi.org/10.1016/j.jddst.2019.101394.
[30] M. Danaei, M. Dehghankhold, S. Ataei, F. Hasanzadeh Davarani, R. Javanmard, A. Dokhani, S. Khorasani, M.R. Mozafari, Impact of particle size and polydispersity index on the clinical applications of lipidic nanocarrier systems, Pharmaceutics 10 (2018) 57, https://doi.org/10.3390/pharmaceutics10020057.
[31] E.B. Souto, J.F. Fangueiro, A.R. Fernandes, A. Cano, E. Sanchez-Lopez, M.L. Garcia, P. Severino, M.O. Paganelli, M.V. Chaud, A. Silva, Physicochemical and biopharmaceutical aspects influencing skin permeation and role of SLN and NLC for skin drug delivery, Heliyon 8 (2022) e08938, https://doi.org/10.1016/j.heliyon.2022.e08938.
[32] A. Javia, A. Misra, H. Thakkar, Design and pharmacodynamic evaluation of DPK-060 loaded nanostructured lipid carrier embedded gel for dermal delivery: a novel approach in the treatment of atopic dermatitis, Colloids Surf. B Biointerfaces 217 (2022) 112658, https://doi.org/10.1016/j.colsurfb.2022.112658.
[33] W. Chaiyana, S. Anuchapreeda, S. Somwongin, P. Marsup, K.H. Lee, W.C. Lin, S. C. Lue, Dermal delivery enhancement of natural anti-ageing compounds from *Ocimum sanctum* Linn. extract by nanostructured lipid carriers, Pharmaceutics 12 (2020) 309, https://doi.org/10.3390/pharmaceutics12040309.
[34] Y. Gilaberte, L. Prieto-Torres, I. Pastushenko, Á. Juarranz, Anatomy and function of the skin, in: Nanoscience in Dermatology, Academic Press, London, UK, 2016, pp. 1–14, https://doi.org/10.1016/b978-0-12-802926-8.00001-x.
[35] R. Hamed, B.J.A. Nahia, A.Z. Alkilani, Y. Al-Adhami, R. Obaidat, Recent advances in microneedling-assisted cosmetic applications, Cosmetics 11 (2024) 51, https://doi.org/10.3390/cosmetics11020051.
[36] M.M. Badran, J. Kuntsche, A. Fahr, Skin penetration enhancement by a microneedle device (Dermaroller) *in vitro*: dependency on needle size and applied formulation, Eur. J. Pharm. Biopharm. 36 (2009) 511–523, https://doi.org/10.1016/j.ejps.2008.12.008.
[37] A. Sabri, J. Ogilvie, J. McKenna, J. Segal, D. Scurr, M. Marlow, Intradermal delivery of an immunomodulator for basal cell carcinoma; expanding the mechanistic insight into solid microneedle-enhanced delivery of hydrophobic molecules, Mol. Pharm. 17 (2020) 2925–2937, https://doi.org/10.1021/acs.molpharmaceut.0c00347.
[38] N. Akombaetwa, A.B. Ilangala, L. Thom, P.B. Memvanga, B.A. Witika, A.B. Buya, Current advances in lipid nanosystems intended for topical and transdermal drug delivery applications, Pharmaceutics 15 (2) (2023) 656, https://doi.org/10.3390/pharmaceutics15020656.
[39] S.G. Lee, J.H. Jeong, K.M. Lee, K.H. Jeong, H. Yang, M. Kim, H. Jung, S. Lee, Y. W. Choi, Nanostructured lipid carrier-loaded hyaluronic acid microneedles for controlled dermal delivery of a lipophilic molecule, Int. J. Nanomedicine. 9 (2013) 289–299, https://doi.org/10.2147/IJN.S54529.
[40] S. Cao, Y. Wang, M. Wang, X. Yang, Y. Tang, M. Pang, W. Wang, L. Chen, C. Wu, Y. Xu, Microneedles mediated bioinspired lipid nanocarriers for targeted treatment of alopecia, J. Control. Release. 329 (2021) 1–15, https://doi.org/10.1016/j.jconrel.2020.11.038.
[41] A. Matta, L.S.L. Janardhanam, V.V.K. Venuganti, Dissolvable layered microneedle patch containing 5-fluorouracil for localized treatment of oral carcinoma, J. Chem. Sci. 135 (2) (2023) 23, https://doi.org/10.1007/s12039-023-02149-2.
[42] T.M.T. Guimarães, T. Moniz, C. Nunes, M.M. Zaharieva, M. Kaleva, K. Yoncheva, H. Najdenski, S.A.C. Lima, S. Reis, Polymeric microneedles for transdermal delivery of rivastigmine: design and application in skin Mimetic model, Pharmaceutics 14 (2022) 752, https://doi.org/10.3390/pharmaceutics14040752.
[43] Y. Wu, L.K. Vora, R.F. Donnelly, T.R.R. Singh, Rapidly dissolving bilayer microneedles enabling minimally invasive and efficient protein delivery to the posterior segment of the eye, Drug Deliv. Transl. Res. 13 (2022) 2142–2158, https://doi.org/10.1007/s13346-022-01190-x.
[44] R.F. Donnelly, D.I.J. Morrow, M.T.C. McCrudden, A.Z. Alkilani, E.M. Vicente-Pérez, C. O'Mahony, P. González-Vázquez, P.A. McCarron, A.D. Woolfson, Hydrogel-Forming and dissolving microneedles for enhanced delivery of photosensitizers and precursors, Photochem. Photobiol. 90 (2013) 641–647, https://doi.org/10.1111/php.12209.
[45] I. Lee, J. He, M. Tsai, K. Lin, Fabrication of a novel partially dissolving polymer microneedle patch for transdermal drug delivery, J. Mater. Chem. B 3 (2) (2015) 276–285, https://doi.org/10.1039/c4tb01555j.
[46] K. Ita, Dissolving microneedles for transdermal drug delivery: advances and challenges, Biomed. Pharmacother. 93 (2017) 1116–1127, https://doi.org/10.1016/j.biopha.2017.07.019.
[47] A. Singh, S. Yadav, Microneedling: advances and widening horizons, Indian Dermatol. Online J. 7 (4) (2016) 244–254, https://doi.org/10.4103/2229-5178.185468.
[48] Q. Yang, W. Zhong, Y. Liu, R. Hou, Y. Wu, Q. Yan, G. Yang, 3D-printed morphology-customized microneedles: understanding the correlation between their morphologies and the received qualities, Int. J. Pharm. 638 (2023) 122873, https://doi.org/10.1016/j.ijpharm.2023.122873.